Chapter 8
Pharmacometrics in Bacterial Infections

Sherwin K. B. Sy and Hartmut Derendorf

8.1 Introduction

The issue of bacterial resistance to antimicrobial agents, which is evident by a diminishing therapeutic value of many commercially available antimicrobials, has reached an alarming height of imminent danger to the general population. The rapid emergence of bacterial resistance to antimicrobial agents has rendered many of the commercially available antibiotics useless at the clinically tolerable dose. The resistance to treatment has also rapidly increased hospital mortality due to opportunistic infections (De Kraker et al. 2011). To combat this crisis, there are two options: (1) the development of new antimicrobials, which requires developing a new class of drugs and/or (2) preserving the value of existing ones by tackling bacterial resistance mechanisms. The first option can prove extremely costly and lengthy; the pharmaceutical industry has no incentive in developing new class of antibiotics due to a small return on the investment. The second option can be addressed in two ways: first, development of new drugs that counter the resistance mechanisms in bacteria for example the use of β-lactamase inhibitor in combination with a β-lactam agent; and second, optimizing treatment of existing antibiotics. The need for an optimized treatment, whether it is for new or existing drugs, in order to limit the chance of bacterial resistance, has prompted the use of quantitative approaches to guide dosing regimens.

The application of pharmacokinetic–pharmacodynamic (PKPD) modeling and simulation has been proven useful in the selection of dosing regimens that overcome resistance development and achieve the desired clinical outcome (Drusano

H. Derendorf (✉)
Department of Pharmaceutics, College of Pharmacy,
University of Florida, Gainesville, FL, USA
e-mail: hartmut@ufl.edu

Sherwin K. B. Sy
Department of Pharmaceutics, University of Florida, Gainesville, FL, USA

S. Schmidt, H. Derendorf (eds.), *Applied Pharmacometrics,* AAPS Advances
in the Pharmaceutical Sciences Series 14, DOI 10.1007/978-1-4939-1304-6_8

2004). Even with a good track record of optimizing antimicrobial dosages, however, the PKPD model and simulation is still underutilized in managing bacterial infections. This chapter focuses on the available PKPD models that were derived from *in vitro*, animal, and clinical data. The discussion separates two major modeling approaches applied to antimicrobial PKPD, namely, the minimum inhibitory concentration (MIC)-based and the *in vitro* time-course-based approaches. We explore how each approach handles monotherapy and combination therapy, as well as in the context of emergence of drug-resistant infections.

8.2 MIC-based Approaches

The PKPD properties of antibiotics to guide dosing schedules were conceived as early as the 1950s by Eagle who demonstrated the time-dependent nature of penicillin antibacterial activity, the concentration-dependent pattern for streptomycin and bacitracin, and a characteristic mixture of both patterns for tetracyclines (Eagle et al. 1950a, b; 1953a, b). With this knowledge, Eagle suggested that the efficacious way to administer penicillin was to give continuous infusion and regimens that gave the highest peak concentrations, such as an intravenous bolus, and would provide an effective cure for drugs that are concentration dependent (Eagle et al. 1950a).

It was not until much later, when Craig rediscovered and expanded the PKPD concepts in antimicrobial therapy using rodent studies (Craig 1998), that the PKPD relationship of new antibiotics was evaluated routinely. This information provides the basis for deciding the dose and dosing interval of antimicrobial agents, as well as determination of susceptibility breakpoints.

This first part of characterizing the PKPD properties of antibiotics is generally classified as the MIC-based approaches. This section will discuss how the MIC-based approaches are utilized to optimize dosing strategies, as well as their limitations.

8.2.1 In Vitro Susceptibility Tests

The MIC has been the primary tool for determining bacterial susceptibility to an antibiotic. This test is carried out by either an agar diffusion or broth dilution; both methods are most commonly used for MIC determination, since they are easy to perform (Jorgensen and Ferraro 2009). In the agar diffusion method, the bacterial culture is spread uniformly across the agar plate and then grown overnight; a rectangular strip impregnated with a gradient amount of drug is laid on top of the agar plate. This test is commonly known as the Epsilometer test (or Etest). Because MICs are typically based on twofold dilution, the drug concentrations on the Etest strip also increases exponentially. In post-24-h incubation, an elliptical zone of bacteria-free area resulted along the strip where the drug concentrations were

sufficient against the specific bacteria. The point at which the bacteria-free ellipse intersects with the Etest strip is the MIC. Older agar diffusion test utilizes disk diffusion wherein circular wafers impregnated with fixed concentrations of antibiotic are placed on a plate full of bacteria.

The broth dilution method utilizes a liquid medium usually Mueller-Hinton broth inoculated with specific bacterial colony forming unit (5×10^5 CFU/mL) and specific drug concentration is pre-added in twofold dilutions (e.g., 0.125, 0.25, 0.5,1, 2, 4, 8,…μg/mL). The mixture is incubated for 24 h at 37 °C. The lowest drug concentration of antibiotic allowing no visible bacterial growth in the media is the MIC. Positive controls containing only the bacteria and negative controls containing only MHB are observed simultaneously. Because the MIC is determined by visual inspection, it does not necessarily mean that there are no bacteria remaining in the media. Rather in most cases, the bacteria level is below a CFU size that is detectable by the human eye ($\leq 10^6$ CFU/mL). For large MIC values (MIC ≥ 100 μg/mL), it is advisable to evaluate susceptibility using a linear increase (e.g., 100, 200, 300,…μg/mL) than an exponential increase (i.e., twofold) in drug concentration.

The macrodilution and microdilution methods differ in the volume of the media wherein macrodilution method is often between 1 and 2 mL and microdilution is ≤500 μL. The bacteria inoculum should be the same for both methods. The volume of bacteria solution to add to the mixture should be adjusted to achieve a final inoculum of 5×10^5 CFU/mL.

For the past several decades, the MIC has been used extensively to define the susceptibility of a specific bacterial species or strain to an antibiotic agent. In the hospital setting where multiple strains of a specific bacterial species are available, MIC_{50} and MIC_{90}, representing the concentration of the antimicrobial agents wherein 50 and 90% of the bacterial population do not show visible growth after 24-h incubation, are often reported (Walkty et al. 2011). The ease of use, rapid turnover of results, and cost effectiveness have made the MIC approach the testing of choice in the clinical setting.

8.2.2 PKPD Indices

The current approach in the treatment of microbial infection in the clinic is primarily based on the relationships between drug exposure and MIC (Drusano 2004; Schmidt et al. 2008). The three standard PKPD indices are $fT > \text{MIC}$, fC_{max}/MIC, and $f\text{AUC}/\text{MIC}$. The duration of time in the 24-h period wherein the drug concentration is above the MIC is $fT > \text{MIC}$. The percentage of time above MIC over the 24-h period is often used instead ($\%fT > \text{MIC}$). AUC refers to the area under the drug concentration–time curve over the 24-h period and C_{max} is the peak drug concentration. The prefix *f* refers to the free drug concentration. The indices are based on the free and unbound drug concentration, as only the unbound drug can exert its pharmacological effect. If the relationship is time dependent, the dosing strategy is simply to maintain the free drug concentrations above the MIC value for an ex-

tended period of time. On the other hand, if the efficacy is concentration dependent, the goal is to attain sufficient peak drug concentrations or drug exposure above MIC (Mueller et al. 2004). The β-lactams are commonly associated with the term "concentration-independent kill" or "time-dependent kill." That is because the efficacy of the β-lactams is associated with the time that the free drug concentration of these agents is maintained above MIC. The quinolones and aminoglycosides, on the other hand, are "concentration dependent" in their effects. Whether these agents are above MIC for an extended period or not do not seem to have a significant impact on the observed antimicrobial effect but rather the magnitude of the peak concentration is associated with a more efficient bacterial kill. The third type of antibiotics which include azithromycin and vancomycin is not concentration dependent but their efficacy is linked to the *f*AUC/MIC ratio (Drusano et al. 2004; Rybak et al. 2009a, b). The 24-h exposure, measured by the AUC-to-MIC (*f*AUC/MIC) ratio, is related to the observed effect. The action of many antimicrobial agents has generally been classified based on these PKPD indices.

The determination of which indices best characterize the drug action is based on fitting a sigmoidal E_{max} model to the PD endpoint such as the bacterial $\log_{10}$ CFU/mL at 24 h or the log change in CFU/mL against the three PK/PD indices (Dudhani et al. 2010). The PD endpoint is often taken from animal studies wherein several live mouse thighs or lungs were injected with specific bacteria with predetermined MIC. The mice were then administered antibiotic at different drug doses and regimens in dose fractionation studies. The pharmacokinetic parameters ($fT>$MIC, fC_{max}/MIC, *f*AUC/MIC) were then determined for each animal. At the end of the experiments, the bacterial CFU/mL was determined from the tissues injected with bacteria. The 24-h $\log_{10}$ CFU/thigh against the PKPD indices was used to evaluate which PKPD index best characterizes the activity of the specific antimicrobial agent being tested (Dudhani et al. 2010). The relationship between the PD endpoints and PKPD indices are plotted and the best fits for the relationships were determined by R^2 (coefficient of determination). It was suggested that the PKPD index determined in mice could be extrapolated to clinical efficacy (Ambrose et al. 2007). Many of the current dosing regimens in the clinic were based on the PKPD indices determined from animal studies. Vancomycin dosing regimens, for example, were determined based on the target of AUC/MIC ratio of approximately 325 in treating ventilator-associated *Staphylococcus aureus* pneumonia (Moise-Broder et al. 2004a, b; Sakoulas et al. 2004; Rybak et al. 2009b). The vancomycin nomogram was designed to achieve a target trough concentration of 15–20 mg/L (Kullar et al. 2011).

Drusano provided an explanation of how the shape of the drug profile affects the type of cell kill for drugs that are concentration dependent versus those that are time dependent (Drusano 2004; Jumbe and Drusano 2011). The rate of kill in concentration-dependent drugs is different at each segment of the concentration–time profile and the total number of organisms killed can be approximated as an expectation which is the summation of the kill rate and time period over the specific kill rate. For time-dependent drugs, the kill rate is constant and the total

cell kill is the rate constant multiplied by the time period that the drug concentration is above the MIC.

8.2.3 Probability of Target Attainment and Clinical Breakpoints

The probability of target attainment (PTA) is often determined from simulation of 1000–10,000 individual drug concentration–time profiles using a population pharmacokinetic model and the proportion of the population above a specific target (Drusano et al. 2001; de Kock et al. 2014). The simulation generates a distribution of PKPD index (e.g., $f\text{AUC}_{24}$/MIC) which becomes the basis for determining the likelihood of achieving a certain target attainment. The $f\text{AUC}_{24}$/MIC will be used as an example because it is easier to generate than $fT > \text{MIC}$ or $f\text{C}_{max}$/MIC, as AUC can be estimated by integrating the population-PK model or estimated from the clearance values without running secondary pharmacokinetic analysis (e.g., noncompartmental analysis) of the generated profiles. The PTA is determined as the proportion of simulated individual profiles that are above a specific target, such as $f\text{AUC}_{24}$/MIC, to achieve greater than or equal to 2 $\log_{10}$ kill from animal studies, for a range of increasing MIC values and is usually evaluated using several dosing regimens in dose fractionation studies. In the study of tigecycline against *E. coli*, Ambrose et al. (2009) determined the potential tigecycline–Enterobacteriaceae susceptibility using both PTA and clinical response expectation as responses. The steady-state AUC_{24} was simulated from the distribution of clearance parameter from a population pharmacokinetic model of tigecycline. In the example in Fig. 8.1,

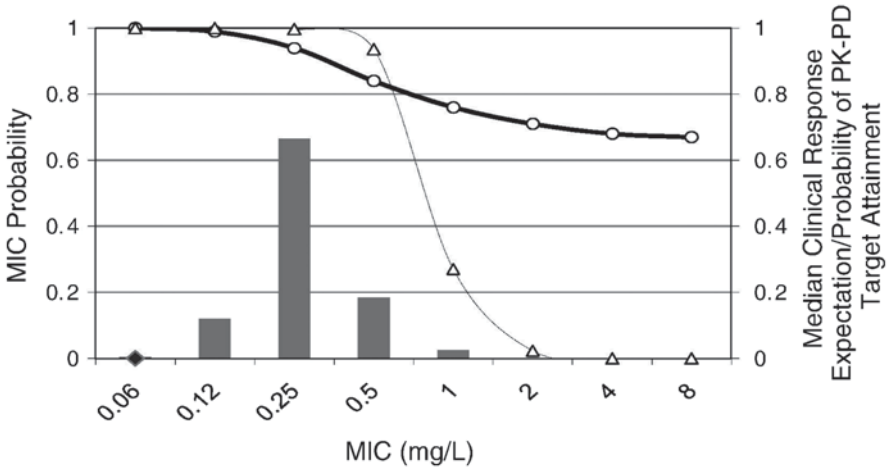

Fig. 8.1 Probability of target attainment (PTA, *open triangles*) based on $\text{AUC}_{ss,24h}$/MIC ratio, clinical response expectation (*open circles*), and tigecycline MIC distribution (*bars*), showing a trend of decreasing PTA and median clinical response expectation in increasing MIC. (Image from Ambrose et al. 2009; used with permission)

PTA is plotted as a function of MIC, represented by triangle symbols. The clinical response expectation versus MIC, represented by circular symbol, was determined from a logistic regression model that describes the PKPD relationship for efficacy in patients with complicated intra-abdominal infections (Meagher et al. 2007; Passarell et al. 2008). As shown in their study, the two metrics, namely PTA and clinical response expectation, may not necessarily correlate with each other. However, both metrics indicate a trend towards less favorable outcome with increasing MIC.

A natural extension of the PTA is to categorize the antimicrobial activity of specific treatment against a microorganism population. The European Committee on Antimicrobial Susceptibility Testing (EUCAST) has provided definitions to categorize microorganisms' antibiotic phenotype based on the quantitative antimicrobial susceptibility evaluation (Kahlmeter et al. 2003, 2006). Mouton et al. (2012) provided this categorical description:

> A microorganism is defined as susceptible by a level of antimicrobial activity associated with a high likelihood of therapeutic success. A microorganism is categorized as susceptible by applying the appropriate breakpoints in a defined phenotypic test system. Conversely, resistance is defined as a high likelihood of therapeutic failure. Ideally, clinical breakpoints should therefore distinguish between patients that are likely or unlikely to respond to antimicrobial treatment.

The clinical breakpoints are determined from (1) statistical approach such as classification and regression tree (CART) analysis or multivariate logistic regression to look for a value of PKPD index that best differentiate failures and successes in treatment outcome and (2) probabilistic approach of PTA that considers the variability in patients' pharmacokinetic and the MIC of the microorganism population. With the probabilistic approach of PTA, the microorganism with MIC values that result in the PKPD index value lower than the target are considered resistant, which translates to a lower probability of cure whereas those that result in a larger PKPD index values than a specific target are considered susceptible. This target value that separates the PKPD index for the two-microorganism phenotype is the clinical MIC breakpoint. It is noted that the clinical breakpoint may be dependent on the dosing regimen. A case is illustrated by Mouton et al. (2005, 2012) wherein the relationship between $fT>\text{MIC}$ and MIC of ceftazidime for two different dosing regimens produces two separate and distinct PTA–MIC curves as shown in Fig. 8.2. Assuming that the target is 60 % $fT>\text{MIC}$, the dosing of 500 mg thrice daily and 1 g thrice daily resulted in breakpoints of 4 and 8 mg/L MIC.

Ambrose et al. (2007) provided an excellent review to show how rodent studies translate to humans. The studies in rodent infection models showed that a total levofloxacin AUC_{24}:MIC value of 88 in immunosuppressed mice was associated with favorable microbiological response (Jumbe et al. 2003). Levofloxacin $f AUC_{24}$:MIC value of 62 determined from patients with hospital-acquired pneumonia separates those patients with 90 and 43 % response to therapy (Drusano et al. 2004).The two studies show a good correlation between rodent studies and humans, given that the PKPD indices in animal studies are closely related to that in humans.

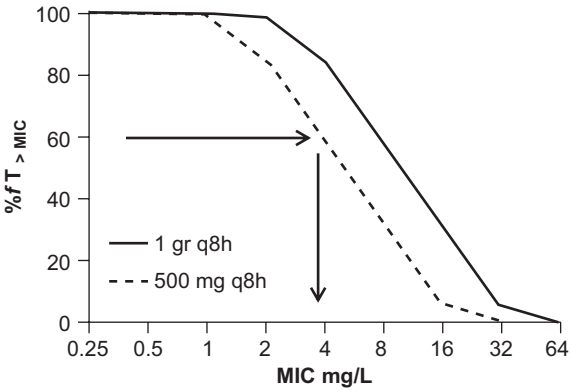

Fig. 8.2 The percent of time that the free ceftazidime concentration is above MIC (%$fT>$MIC) for two dosing regimens of ceftazidime (1 g q8h vs. 500 mg q8h) against MIC to illustrate that clinical breakpoint is dependent on the dosing regimen. *Arrows* indicate that the pharmacodynamics target corresponding to 60 %$fT>$MIC is 4 and 8 mg/L for 500 mg q8h and 1 g q8h, respectively. (Image from Mouton et al. 2012; used with permission)

8.2.4 Limitations of the MIC-based Approach

Though this approach has been used to guide dosing for various classes of antimicrobials, several shortfalls of the MIC-guided approach are discussed here. The determination of the MIC of the patient's infection often takes several days following the initial treatment and consequently the drug concentration and duration may not be optimal without the prior knowledge of the MIC, particularly when using the relationship between pharmacokinetic properties of the drug and the MIC-based PKPD indices to guide treatment. This simplification of dosing scheme is believed to potentially lead to treatment failure and may foster the emergence of resistant bacterial populations (Hoffman and Stepensky 1999).The utility of MIC assumes that this value is stationary. This is not the case because MIC within a bacteria species can change. When bacteria are exposed to a low concentration of drug, which is not enough to eradicate them, the bacteria will acquire resistance, resulting in a shift towards a higher MIC level (Tam et al. 2007a). Also depending on the species and strain of bacteria, the MIC may not be consistent across the species and strains. This scenario renders a "nonstationary" MIC. With an increasing rate of treatment failure, MIC is more likely to be changing over time due to development of resistance. For example, the AmpC β-lactamase is induced when exposed to low β-lactam concentration. The *ampC* expression is repressed by three AmpD homologues, including the previously described AmpD protein (Langaee et al. 1998, 2000) plus two additional proteins AmpDh2 and AmpDh3 (Juan et al. 2006). The two additional homologues are responsible for the stepwise *ampC* upregulation that results in hyper-expression of cephalosporinase and high level of β-lactam resistance (Juan et al. 2006).

The rate of bactericidal activity or bacteriostatic effect with different drug concentrations cannot be determined from the MIC approach. Several killing patterns can converge to the same MIC value when only the 24-h time point is measured. Relying on a "snapshot" view of MIC for defining the PKPD relationship for the entire treatment duration can be misleading.

Because only unbound drug concentration can exert its pharmacological effect, ignoring protein binding and tissue distribution of the drug can have serious implication in extrapolating *in vitro* efficacy results to human studies. When the drug enters the blood stream, it can bind to proteins such as albumin, α-, β-, or γ-globulins, α1-acid glycoprotein, lipoproteins, and/or erythrocytes (Dasgupta 2007; Treyaprasert et al. 2007; Mouton et al. 2008). The percentage of drug binding can be constant (linear) or nonconstant (nonlinear) depending on the drug concentration; characterization of protein binding across a range of drug concentrations can provide important information on its protein binding properties. Since anti-infective drugs need to get to the infection sites, for example, in skin infection, the unbound fraction of drug crosses the membrane to the infected tissue. Microdialysis procedures have been used to determine the free fraction of drug at a specific tissue (e.g., adipose and skin; Li et al. 2006). It is important to consider protein binding when translating *in vitro* results to the clinic.

8.2.5 Resistance Problem in Antimicrobial Therapy

The number of new bacterial strains with more efficient resistance mechanisms has emerged over the past decade. From the year 2000 through 2004, the percentages of methicillin susceptible and resistant *S. aureus* (MSSA and MRSA) isolates with vancomycin MIC of 1 μg/mL increased from 40 to >70% and from 10 to >60%, respectively (Wang et al. 2006). Within the span of 5 years, *S. aureus* clinical isolates have evolved towards decreasing vancomycin susceptibility. The resistance problem is not isolated to just one class of antimicrobials. Various newly discovered β-lactamases can rapidly inactivate β-lactams and some β-lactamases such as the variant of TEM-1 are resistant to β-lactamase inhibitors, for example clavulanic acid (Sideraki et al. 2001).

There are experimental evidences that the efflux pump upregulation is a first-line defense for microorganisms when challenged with antimicrobial agents (Jumbe et al. 2006; Louie et al. 2007; Drusano et al. 2009). The MexCD-OprJ, not typically expressed under noninduced conditions, exports fluoroquinolones and a number of β-lactams (Poole et al. 1996; Masuda et al. 2000b). MexXY-OprM contributes to resistance to fluoroquinolone, aminoglycoside, and some β-lactam (Aires et al. 1999; Mine et al. 1999; Masuda et al. 2000b; Sobel et al. 2003); this efflux pump is induced by tetracycline and aminoglycosides (Aires et al. 1999; Mine et al. 1999; Masuda et al. 2000a). β-Lactam resistance in clinical isolates of *Pseudomonas aeruginosa* has been shown to interplay between diminished production of OprD (an outer membrane protein that regulates the entry of carbapenems) and an increased AmpC β-lactamase activity (Quale et al. 2006).

The choice of dosing regimen affects the extent of resistance development. Tam et al. (2007a) demonstrated that the relationship between quinolone exposure and resistance amplification is characterized by an inverted U-shaped curve. This indicates that development of resistance is minimal at low antimicrobial challenge and rapidly increases over a range of drug concentration unless a sufficiently high

drug concentration kills both the susceptible and resistant populations. These results prompted recommendations for increasing doses, shorter treatment period, and combining several antimicrobials with different mechanisms of action to counter the emergence of drug-resistant bacteria (Mouton et al. 2011).

8.2.6 Combination Therapies

The resistance to treatment has also rapidly increased hospital mortality due to opportunistic infections (De Kraker et al. 2011). Administering two antibiotic drugs with different mechanisms of action can potentially restore the utilities of these agents. This approach is called combination therapy. The action of many antimicrobial agents has generally been classified based on the PKPD indices, previously described. These indices, however, are relevant primarily to monotherapy. When evaluating combination therapy that includes multiple antibiotics, the pattern may no longer be relevant. This renders the classification of combination therapy and the determination of optimal dosing strategies nontrivial.

Drugs of different mechanisms of action may act synergistically, resulting in greater than fourfold decrease in the MIC of each drug in the same pathogen *in vitro* (Paul et al. 2004). The use of aminoglycoside/β-lactam combination was practiced in the past (Piccart et al. 1984; Hoepelman et al. 1988a, b; Mondorf et al. 1989). However, the benefits from the combination were later questioned based on a meta-analysis study (Bliziotis et al. 2005). The likely reason could be that the patients who received combination therapy had a higher propensity for mortality since combination antibiotics are more commonly prescribed for the critically ill patients than the single-agent antibiotics. The one subgroup of Gram-negative pathogens, for which the question of combination therapy is currently being investigated in more and more studies, is *P. aeruginosa* (Louie et al. 2013). This bacterial species is also more common in patients who are severely ill, including the late stage of morbidity in cystic fibrosis (CF) patients (Breen and Aswani 2012). In fact, the Cystic Fibrosis Foundation guidelines recommend that an antipseudomonal β-lactam with an aminoglycoside be used in the treatment of acute pulmonary exacerbations of CF (Flume et al. 2009). CF patients were thought to have higher clearance and larger volumes of distribution, which makes dosing more challenging due to lower exposure (Spino 1991). In a matched control study, no difference was found in aztreonam volume of distribution between CF patients and matched healthy subjects but total body clearance was 30% higher in CF patients due to enhanced renal clearance as CF patients had 20% higher free fraction of the drug (Vinks et al. 2007).

The synergy of activities from combination of β-lactam and aminoglycoside would be particularly beneficial in these difficult-to-treat populations. The combination of an aminoglycoside and a β-lactam seems to be the most frequently used combination against *P. aeruginosa*. Louie et al. (2013) showed that tobramycin in combination with meropenem suppressed resistance amplification in *P. aeruginosa* at all combination regimens that were tested in the murine pneumonia model.

Safdar et al. (2004) performed a meta-analysis on combination antimicrobial therapy for bacteremia due to Gram-negative bacilli. Their overall results, combining all types of bacteria that were found in their literature search, indicated that combination therapy does not reduce mortality in patients with Gram-negative bacteremia. One limitation of their study was that the literature that they used did not stratify the outcome by the severity of illness. The patients with multiple comorbidities were also more likely to die due to their underlying conditions. In a stratified analysis, they found a significant survival benefit with combination therapy in *P. aeruginosa* bacteremia, translating to an approximately 50% mortality reduction (CI: 32–79%). This specific result provided the rationale for the hypothesis that the combination of aminoglycoside and β-lactam may provide synergism *in vivo* in a setting where the suspected infection is predominantly *P. aeruginosa* or other multiresistant Gram-negative bacilli where more than one drug would assure susceptibility to at least one of the antimicrobial agents.

The exact mechanism of action of aminoglycosides is not fully known. It was suggested that aminoglycosides could be either bacteriostatic and/or bactericidal (Bakker 1992). The bacteriostatic effect stops the growing of bacteria by inhibiting protein synthesis as the aminoglycoside binds to the 16S rRNA. The mechanism for its bactericidal effect is by disrupting the integrity of bacterial cell membrane (Shakil et al. 2008). In contrast, the mechanism of action of β-lactam antibiotics is completely known. β-Lactam antibiotics are bactericidal and act by an irreversible inhibition of the penicillin-binding proteins, which normally catalyze the cross-linking of bacterial cell walls. The drug binding to the penicillin-binding proteins kills the bacteria due to the disruption of the cell wall synthesis (Fisher et al. 2005).

The PKPD indices for combination therapy have not been explored yet. It is likely more challenging to develop since the evaluation would require a much larger set of dose fractionation studies especially combining two drugs. The *in vitro* time-course-based approach may provide a simpler methodology to evaluate dosing regimens for combination therapies than the summary PKPD variables that are MIC based.

8.3 *In Vitro* Time-Course-Based Approaches

8.3.1 Time-Kill Kinetic Studies

The advancement of PKPD modeling approach came with more defined *in vitro* methodologies. The *in vitro* time course of drug–bacterial response characterized by the kill-curve assays has been used as the basis for developing PKPD models to describe bacterial population dynamics, drug effects, and the emergence of resistance. Depending on the objective of the study, the drug concentration in these *in vitro* time-kill experiments can be relatively constant in the static situation (Garrett et al. 1966; Mielck and Garrett 1969; Garrett and Nolte 1972) or dynamically changing to mimic the *in vivo* half-life of the drug in humans (Sanfilippo and Morvillo 1968;

Sanfilippo and Schioppacassi 1973; Grasso et al. 1978). The data from static time-kill experiments are often used to develop a mathematical model that links the free drug concentrations to the bacterial response whereas dynamic time-kill data are used to validate the model and to predict the outcome in the clinic. The dynamic kill-curve provides an alternative for evaluating PKPD relationships; it simulates the time course of the unbound drug concentrations at the site of action based on a preset half-life. Using multiple pumps, the hollow fiber infection model is used to simulate concentration-time profiles of free drug concentration that mimics the *in vivo* profiles (Crandon et al. 2012). The effects of different dosing regimens, drug half-lives and even starting inocula can be simulated to study their effects on the bacterial population dynamics over a time period, for example 24 or 48 h.

8.3.2 PKPD Models of In Vitro Time-Kill Kinetics

The Logistic Growth Models The PKPD models currently used to describe the *in vitro* bacterial population dynamics came from models used to study human population dynamics. In 1838, Pierre-François Verhulst described the logistic growth model that many of the modern antimicrobial PKPD models were based on:

$$\frac{dN}{dt} = r\left(1 - \frac{N}{K}\right)N, \tag{8.1}$$

where N is the population number, r is the growth rate, and K is the carrying capacity or the maximum number of individuals that is supported by the environment (Gershenfeld 1999). The analytical solution to Eq. (8.1) is:

$$N(t) = \frac{KN_0e^{rt}}{K + N_0(e^{rt} - 1)}, \tag{8.2}$$

where N_0 is the initial population number at time $t=0$. The important property of this model is that the limit of this function as time goes to infinity is the carrying capacity: $\lim_{t\to\infty} N(t) = K$. In an *in vitro* time-kill curves of both static and dynamic systems, the bacterial CFU is restricted from growing indefinitely and usually reaches a plateau, where the net growth is zero. For this reason, the logistic growth model suitably describes this behavior.

The Compartmental Models The second type of antimicrobial PKPD model can be described in simplistic terms consisting of the natural self-replication and death of bacteria (Eq. 8.3):

$$\frac{dN}{dt} = (k_{\text{growth}} - k_{\text{death}})N, \tag{8.3}$$

where N is the bacterial population with the initial count of N_0, k_{growth} is the first-order rate constant for bacterial synthesis, and k_{death} is the first-order rate constant for bacterial death. This common structure to describe bacterial growth is also used in other disease areas such as tumor dynamic models, where a first-order self-replication rate is implemented (Jusko 1971). This model assumes that the bacteria are from a homogeneous population with the same growth and death rate constants, which may not reflect the true population of microbes, which is known to select for resistant strain in the presence of an antimicrobial challenge. The variations based on the compartmental model have improved on this limitation and will be described more thoroughly in later sections of this chapter.

The Mechanistic Models The third type of antimicrobial models considers the bacterial growth cycle, states of bacterial susceptibility, drug–receptor interaction, and the mechanisms of drug action. This type of models utilized many concepts of mathematical modeling in biology, including the two modeling approaches discussed above. Each of the mechanistic models will be discussed separately as there is no common mathematical approach across these models that can be summarized briefly.

8.3.3 Modifications on the Logistic Growth Model

To incorporate drug action to the capacity limited growth model, Eq. (8.1) can be modified to include a function to describe the drug effect:

$$\frac{dN}{dt} = k_{growth} N\left(1 - \frac{N}{N_{max}}\right) - f_{death}(\text{drug}), \tag{8.4}$$

where the added f_{death} (drug) describes the effect of an antimicrobial agent (Nolting et al. 1996; Mouton et al. 1997; Yano et al. 1998; Mouton and Vinks 2005). In this equation, as N approaches N_{max}, the growth term approaches a plateau or stationary condition, where there is no net change in the bacterial population. The drug effect is often represented by an E_{max} or a sigmoidal E_{max} model such that,

$$f_{death}(\text{drug}) = \frac{E_{max} C^{\gamma}}{EC_{50}^{\gamma} + C^{\gamma}} N, \tag{8.5}$$

where C is the drug concentration at any specific time, E_{max} is the maximum drug effect, and EC_{max} is the concentration at which the half-maximum effect is achieved. The shape parameter γ is 1 in the E_{max} model and is a parameter in the sigmoidal E_{max} model.

During the initial growth phase where $N << N_{max}$ and the growth is linear, Eq. (8.4) can be simplified to the following equation (Nolting et al. 1996):

$$\frac{dN}{dt} = \left[k_{\text{growth}} - \frac{E_{\max} C^{\gamma}}{EC_{50}^{\gamma} + C^{\gamma}} \right] N. \tag{8.6}$$

By solving for the analytical solution to Eq. (8.6), one can determine the number of bacteria at time (t) through the following equation:

$$N(t) = N_0 e^{\left(k_{\text{growth}} - \frac{E_{\max} C^{\gamma}}{EC_{50}^{\gamma} + C^{\gamma}} \right) t}. \tag{8.7}$$

Mouton and Vinks proposed that the stationary concentration (SC), which is defined as the concentration at which the growth rate equals the kill rate and is also the point at which no net change in the number of bacteria is observed, can be derived from Eq. (8.7) (Mouton and Vinks 2005). By taking the natural log of the ratio $N(t)/N_0$ divided by time, which is equivalent to $k_{\text{growth}} - \frac{E_{\max} C^{\gamma}}{EC_{50}^{\gamma} + C^{\gamma}}$, one can obtain the equation for C:

$$C = EC_{50} \left[\frac{k_{\text{growth}} - \frac{1}{t} ln \frac{N(t)}{N_0}}{E_{\max} - \left(k_{\text{growth}} - \frac{1}{t} ln \frac{N(t)}{N_0} \right)} \right]^{\frac{1}{\gamma}}. \tag{8.8}$$

When there is no net change in the number of bacteria, the term $\frac{1}{t} ln \frac{N(t)}{N_0}$ approaches 0 and the SC is defined as:

$$SC = EC_{50} \left[\frac{k_{\text{growth}}}{E_{\max} - k_{\text{growth}}} \right]^{\frac{1}{\gamma}}. \tag{8.9}$$

The SC is not to be confused with the MIC, as SC refers to the concentration where no net bacterial growth occurs. It is often assumed that bacterial growth occurs when the drug concentration is below the MIC. Mouton and Vinks had shown that a correction factor to the SC equation might be required to estimate the MIC (Mouton and Vinks 2005):

$$MIC = EC_{50} \left[\frac{k_{\text{growth}} - 0.29}{E_{\max} - (k_{\text{growth}} - 0.29)} \right]^{\frac{1}{\gamma}}. \tag{8.10}$$

The value 0.29 is obtained from the kill curves such that $N(t)$ reached 10^8 CFU/mL at 18 h, assuming an initial inoculum of 5×10^5 CFU/mL. This correction factor

is therefore dependent on the specific system that is being tested. The relationship between MIC and SC is described in greater detail in Mouton and Vinks (2005).

Tam et al. (2008) modified the logistic growth model to study the effects of gentamicin and amikacin on the *in vitro* time-kill kinetics of *P. aeruginosa* ATCC 27853 and *Acinetobacter baumannii* ATCC BAA 747, respectively, by introducing an adaptation factor to the EC_{50} parameter:

$$f_{\text{death}}(\text{drug}) = \frac{E_{\max} C^{\gamma}}{(\propto EC_{50})^{\gamma} + C^{\gamma}} N \tag{8.11}$$

α is defined as:

$$\propto = 1 + \beta(1 - e^{-C\tau t}), \tag{8.12}$$

where τ is the exponent of the adaptation factor and β is the maximal adaptation. The range of values for the function $1 - e^{-C\tau t}$ is between 0 and 1. The adaptation function α starts from a baseline EC_{50} and increases over time to a maximal value of β, if τ is positive.

Delay functions were applied to both the growth rate and the drug effect function to describe the population dynamics of *Streptococcus pneumoniae, Haemophilus influenzae,* and *Moraxella catarrhalis* in the presence of azithromycin (Treyaprasert et al. 2007). The delay function has the following form:

$$\frac{dN}{dt} = \left[k_{\text{growth}} \left(1 - \frac{N}{N_{\max}} \right) (1 - e^{-xt}) - \left(\frac{k_{\max} C}{EC_{50} + C} \right) (1 - e^{-yt}) \right] N. \tag{8.13}$$

One can see that the delay function has a similar form to the adaptation function discussed above. The two equations, $1 - e^{-xt}$ and $1 - e^{-yt}$ (Mouton et al. 1997), behave like a cumulative density function starting from 0 at $t = 0$ to a maximum value of 1 as $t \to \infty$. The delay function acts as a modulator to allow the curves to conform to the S-shaped pattern of bacterial growth which is often observed during the first couple of hours of the time-kill kinetic experiments in the presence of low antimicrobial agent concentrations. The two functions also shape the transition to plateau after a decrease then increase in bacterial population at the antimicrobial concentrations that allow for bacterial regrowth to occur. An example of model using the delay function is shown in Fig. 8.3. Another modification introduced a second compartment for the persistent bacterial population to differentiate from the first compartment of susceptible bacteria; this alteration was used to model the effect of oxazolidinone on *Staphylococcus aureus* (Schmidt et al. 2009).

Bulitta et al. (2009) linked the bacterial population dynamic to cell wall synthesis, and drug effect of ceftazidime on cell wall synthesis to describe the lag time in bactericidal effect of β-lactams. The study examines the inoculum effect of ceftazidime against *P. aeruginosa*. The natural first-order death rate was dependent on the number of existing CFU in the system and the logistic growth part of the model

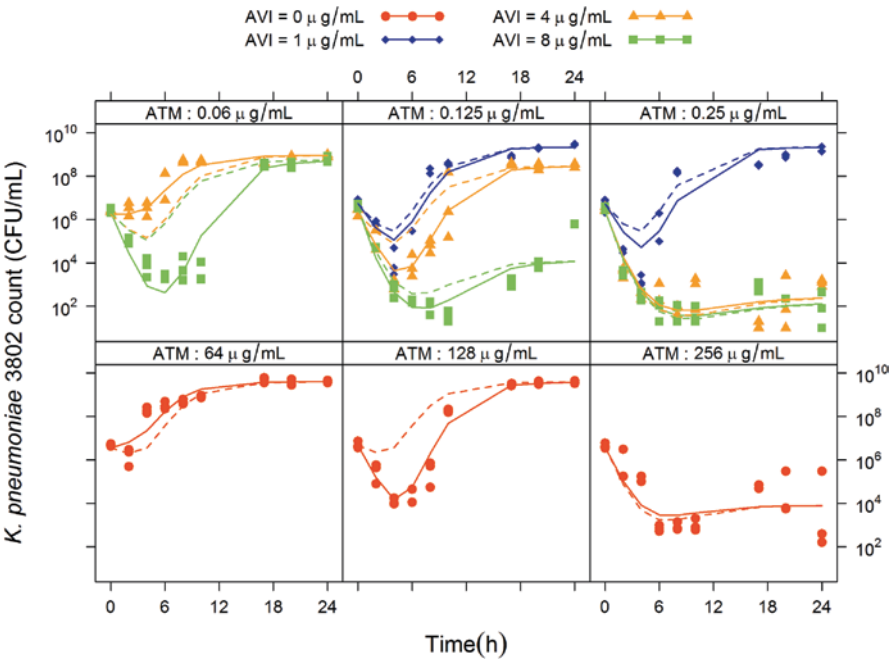

Fig. 8.3 Time-kill kinetics and model prediction of aztreonam-avibactam effect against *K. pneumoniae*

was dependent on both the cell wall synthesis and CFU. The drug effect acts on the compartment representing the cell wall dynamics, since the primary mode of action of ceftazidime is to inhibit cell wall synthesis:

$$\frac{dCW}{dt} = \left[\left(1 - \frac{C_B}{IC_{50,CW} + C_B}\right) - CW\right] \cdot k_{\text{out},CW} \tag{8.14}$$

$$\frac{dN}{dt} = \left[k_{\text{growth}}\left(1 - \frac{N}{N_{\max}}\right)CW - k_{\text{death}}\right]N, \tag{8.15}$$

where CW represents a hypothetical cell wall measurement, whose synthesis is expressed as a fraction of the baseline value. The $IC_{50,CW}$ is the concentration of ceftazidime in the broth that inhibits 50% of cell wall synthesis and $k_{\text{out},CW}$ is the first-order rate constant for the cell wall turnover. The investigators claimed that this model accounts for the slow onset due to the delay between ceftazidime binding to the penicillin-binding proteins and the depletion of cell wall components (Bulitta et al. 2009).

8.3.4 Examples of the Compartmental Model

During the linear growth phase just before reaching the plateauing phase, the population dynamics can be described by simple first-order growth and death rates that are dependent on the bacterial burden present at the specific time. In addition to the logistic growth model, other strategies had been utilized to describe the decrease in the net growth rate as the system approaches the plateau wherein the net bacterial growth is zero. One approach is to implement a phenotypic switch between susceptible and persistent population such that the persisters have a markedly reduced growth rate (Balaban et al. 2004). The overall change in the total number of bacteria would then be the sum of those in susceptible (S) and in persistent resting (R) states, such that:

$$A_{\text{total}} = S + R \tag{8.16}$$

The transition between the two states is defined by their respective rate constants. Nielsen et al. presented an example of compartmental model wherein a two-compartment model was used to describe the *in vitro* effect of a number of antibiotics, including moxifloxacin, vancomycin, benzylpenicillin, cefuroxime, and erythromycin against *Streptococcus pyogenes* (Nielsen et al. 2007). The delay in the effect of drugs was modeled using an effect compartment model for the drug. The following assumptions were made: (1) The drug effect is to increase the death rate of the susceptible state and (2) the antimicrobials have no effect on the persistent population. The differential equations for the two bacterial populations are shown in the following equations:

$$\frac{dS}{dt} = k_{\text{growth}} S - k_{\text{death}} S - k_{SR} S + k_{RS} R \tag{8.17}$$

$$\frac{dR}{dt} = k_{SR} S - k_{RS} R - k_{\text{death}} R. \tag{8.18}$$

As the persistent population is unlikely to return to the susceptible state for the duration of the experiment, the transfer rate for the return to the susceptible state was assumed to be negligible and k_{RS} was fixed to 0. The transfer rate constant that indicates the rate of change from the susceptible to the persistent states, k_{SR}, dictates the growth-limited capacity using the following equation:

$$k_{SR} = \frac{k_{\text{growth}} - k_{\text{death}}}{B_{\max}} (S + R), \tag{8.19}$$

where $B_{\max}$ is the maximum number of bacteria supported by the system.

The investigators evaluated whether the drug decreases the growth rate or increases the rate of death. The later scenario, increase in death rate, was examined as either an additive or a proportional effect. The equations to describe the three different scenarios are shown below:

$$\frac{dS}{dt} = k_{\text{growth}}(1 - f(\text{drug}))S - k_{\text{death}}S - k_{SR}S + k_{RS}R \tag{8.20}$$

$$\frac{dS}{dt} = k_{\text{growth}}S - (k_{\text{death}} + f(\text{drug}))S - k_{SR}S + k_{RS}R \tag{8.21}$$

$$\frac{dS}{dt} = k_{\text{growth}}S - k_{\text{death}}(1 + f(\text{drug}))S - k_{SR}S + k_{RS}R, \tag{8.22}$$

where $f(\text{drug})$ is a sigmoidal $E_{\max}$ model to account for the effect of various drug concentrations.

In a follow-up study, the same group described a mechanism for adaptive resistance in *E. coli* due to gentamicin by introducing two additional compartments that regulate resistance development (Mohamed et al. 2012):

$$\frac{dAR_{\text{off}}}{dt} = k_{\text{off}}AR_{\text{on}} - k_{\text{on}}AR_{\text{off}}C \tag{8.23}$$

$$\frac{dAR_{\text{on}}}{dt} = k_{\text{on}}AR_{\text{off}}C - k_{\text{off}}AR_{\text{on}}, \tag{8.24}$$

where AR_{off} represents the adaptive resistance in dormant stage and AR_{on} is for the active state; the transfer between states is represented by k_{off} and k_{on}; and C refers to gentamicin concentration. A greater flexibility was achieved by the two additional compartments as can be seen in how the model adapted to the data trend. The investigators noted that the model is suitable for gentamicin in the context of compartmental models.

8.3.5 Examples of Mechanistic Models

A similar approach to the compartment model involving three-state susceptibility was used to study colistin effect in *P. aeruginosa* (Bulitta et al. 2010). In this model, the states of susceptibility included susceptible (S), intermediate (I), and resistant (R). A fourth compartment or state ($CFU_{S,lag}$) was introduced to account for the difference between the initial total bacterial burden, CFU_{ALL}, and the initial conditions of the susceptible, intermediate and the resistant populations.

$$CFU_{\text{ALL}} = CFU_{S,lag} + CFU_S + CFU_I + CFU_R. \tag{8.25}$$

The intermediate and resistant populations were assumed to be fractions of the initial total bacterial burden, CFU_0:

$$\frac{dCFU_{S,\text{lag}}}{dt} = (-k_{\text{lag}} - INH_{\text{Kill}} \cdot \leq k_{2S} \cdot C_{\text{Colistin,eff}}) \cdot CFU_{S,\text{lag}} \tag{8.26}$$

$$\frac{dCFU_S}{dt} = \left(\frac{INH_{\text{Rep}} \cdot VG_{\max,S}}{CFU_m + CFU_{\text{ALL}}} - k_d - INH_{\text{Kill}} \cdot k_{2S} \cdot C_{\text{Colistin,eff}} \right) \cdot CFU_S + k_{\text{lag}} \tag{8.27}$$

$$\frac{dCFU_I}{dt} = \left(\frac{INH_{\text{Rep}} \cdot VG_{\max,I}}{CFU_m + CFU_{\text{ALL}}} - k_d - INH_{\text{Kill}} \cdot k_{2I} \cdot C_{\text{Colistin,eff}} \right) \cdot CFU_I \tag{8.28}$$

$$\frac{dCFU_R}{dt} = \left(\frac{INH_{\text{Rep}} \cdot VG_{\max,R}}{CFU_m + CFU_{\text{ALL}}} - k_d - INH_{\text{Kill}} \cdot k_{2R} \cdot C_{\text{Colistin,eff}} \right) \cdot CFU_R, \tag{8.29}$$

where $VG_{\max}$ refers to the maximal rate of bacterial growth in the unit of CFU/(mL.h), CFU_m is the bacterial density that produces 50% of the maximal growth rate, k_{d} is the natural death rate, k_{lag} represents the first-order growth rate constant associated with the slower initial growth phase of the susceptible population in the lag compartment, INH_{Kill} and INH_{Rep} are represented by the following equations:

$$INH_{\text{Kill}} = 1 - I_{\max,\text{Kill}} \cdot \frac{C_{\text{Signal}}}{IC_{50} + C_{\text{Signal}}} \tag{8.30}$$

$$INH_{\text{Rep}} = 1 - I_{\max,\text{Rep}} \cdot \frac{C_{\text{Signal}}}{IC_{50} + C_{\text{Signal}}}. \tag{8.31}$$

INH_{Kill} and INH_{Rep} are inhibition of killing and of replication by signal molecules, C_{signal}. The synthesis of freely diffusible signal molecules C_{Signal} by the bacteria was assumed to inhibit or to slow down the killing effects of colistin. The $I_{\max,\text{Kill}}$ and $I_{\max,\text{Rep}}$ were the maximum inhibition of killing and of replication; the concentration of signal molecules to achieve 50% of the maximum inhibition is the IC_{50}. The kinetic behavior of the hypothetical signal molecule is described by the following differential equation:

$$\frac{dC_{\text{Signal}}}{dt} = \left(CFU_{\text{ALL}} \frac{ml}{CFU} - C_{\text{Signal}} \right) k_{\text{deg}}, \tag{8.32}$$

where k_{deg} is the degradation rate constant.

The assumption was made that the effect of colistin is to displace competitively both Mg^{2+} and Ca^{2+} from the binding sites in the outer membrane and the resulting displacement is responsible for colistin killing effect. The model utilizes receptor occupancy model to describe the competitive inhibition of colistin with Mg^{2+} and Ca^{2+} for the membrane binding sites. The fractional occupancy of these cations as a function of the molar sum of Mg^{2+} and Ca^{2+} concentrations as well as colistin concentration in mg/L is defined such that:

$$Fr_{\text{Cations}} = \frac{C_{\text{Cations}}}{K_{d,\text{Cations}} + C_{\text{Cations}} + \frac{K_{d,\text{Cations}}}{K_{d,\text{Colistin}}} \cdot \frac{C_{\text{Colistin}}}{M_m}}, \tag{8.33}$$

where $K_{d,Cations}$ and $K_{d,Colistin}$ are the dissociation constants for the two cations and colistin, respectively; M_m is the average molecular mass of colistin A and B, which are the two primary components of colistin; and C refers to the concentration of the respective components in the broth. The fraction of the receptors that were not bound to Mg^{2+} or Ca^{2+} was used to compute the effective colistin concentration at the target site. The effective colistin concentration, $C_{\text{Colistin,eff}}$, was a Hill function dependent on the Fr_{Cations} and colistin concentration in broth, C_{Colistin}:

$$C_{\text{Colistin,eff}} = \frac{(1 - Fr_{\text{Cations}})^{\gamma}}{EC_{50}^{\gamma} + (1 - Fr_{\text{Cations}})^{\gamma}}. \tag{8.34}$$

An important difference between this model and the logistic growth or the compartment models is that it assumes that the drug has an effect on all types of bacteria from the susceptible to the intermediate to the resistant ones. The limitation of such a complex model is that the data from an *in vitro* time-kill study will not be sufficient to characterize the model parameters and that many of the parameter values will have to be derived from the literature.

Another compartmental-type model incorporated mechanisms involved in the life cycle of bacterial replication, autolysis, and ceftazidime effect against *P. aeruginosa* (Bulitta et al. 2009). The model utilizes a two-compartment model for the bacteria population and a turnover model to describe the time-kill behavior in the presence of antimicrobial agents. The bacterial life-cycle model utilizes two states for the susceptible population, wherein the first state, S_1, describes the cycle immediately after cell replication whereas the second state, S_2, occurs just before replication:

$$\frac{dS_1}{dt} = 2\left[1 - \frac{CFU_{\text{total}}}{CFU_{\text{total}} + CFU_{\max}}\right]\left[1 - ALys_S\right] \cdot k_{21} \cdot S_2 - Inh_{k12} \cdot k_{12} \cdot S_1 \tag{8.35}$$

$$\frac{dS_2}{dt} = -k_{21} \cdot S_2 + Inh_{k12} \cdot k_{12} \cdot S_1, \tag{8.36}$$

where k_{12} and k_{21} are first-order transition rates between the first and second states. k_{12} is determined from the mean generation time (MGT) such that $k_{12} = 1/MGT_{12}$. The MGT is discussed later in this section. Inh_{k12} is identical to Eqs. (8.30) and (8.31). The factor 2 was used to represent bacterial doubling during cell replication. The autolysin activity $ALys_S$ is stimulated by ceftazidime and is described by a turnover model:

$$\frac{dALys_S}{dt} = \left[\frac{S_{\max,S} \cdot C_B}{SC_{50} + C_B} - \left(1 + \frac{S_{\max,\text{loss}} \cdot C_{Sig1}}{C_{50,\text{Sig}} + C_{\text{Sig1}}}\right) \cdot ALys_S\right] \cdot k_{\text{out}}. \tag{8.37}$$

The $S_{\max,S}$ value limits the maximum value of $ALys_S$ to 1, indicating that a high drug concentration can completely inhibit replication. SC_{50} refers to the drug concentration at which autolysin is half maximally stimulated. $S_{\max,\text{loss}}$ represents the

maximum extent of the inoculum effect at high signal molecule concentrations. In contrast to the previous model, the current one assumes two signal molecules with the following behavior:

$$\frac{dC_{\text{Sig1}}}{dt} = (CFU_{\text{ALL}} - C_{\text{Sig1}}) \cdot k_{\text{deg}} - k_{S12} \cdot C_{\text{Sig1}} + k_{S21} \cdot C_{\text{Sig2}} \tag{8.38}$$

$$\frac{dC_{\text{Sig2}}}{dt} = k_{S12} \cdot C_{\text{Sig1}} - k_{S21} \cdot C_{\text{Sig2}},$$

where the initial conditions for C_{Sig1} and C_{Sig2} were CFU_0 and $CFU_0 \cdot k_{S12} / k_{S21}$. The role of the first signal molecule C_{Sig1} is to slow down the replication rate and C_{Sig1} is in equilibrium with C_{Sig2}.

The life-cycle growth model involving two-stage susceptibility was applied to the study of linezolid against vancomycin-resistant *enterococci* and *S. aureus* (Tsuji et al. 2012a, b). Linezolid effect was assumed to inhibit protein synthesis; a turnover-type model was used to describe its effect:

$$\frac{dP}{dt} = k_{\text{Prot}} \left[\left(1 - \frac{C_{\text{drug}}}{IC_{50} + C_{\text{drug}}} \right) - P \right], \tag{8.39}$$

where P represents the protein pool whose steady-state maximum value is 1, IC_{50} is the linezolid concentration that produces half-maximum inhibition of protein synthesis and k_{prot} is the turnover rate constant of the protein pool. The probability of death due to lack of protein represented by ($Lack = 1 - P$) was defined by the following function:

$$Prob_{\text{death}} = I_{\text{max,Rep}} \cdot Lack. \tag{8.40}$$

The E_{max}-type model was used to describe the plateau phase of the primary susceptible bacterial population. A two-state susceptibility bacterial population was described for S_1 and S_2, similar to the model described in Eqs. (8.35) and (8.36), with the function $1 - Prob_{\text{death}}$ replacing the $1 - ALys_s$ and Inh_{12} was fixed to 1. The number of sensitive alleles (N_{Sen}) was a covariate to determine the IC_{50} of linezolid in inhibiting protein synthesis:

$$IC_{50} = IC_{50\text{Sen}0} \cdot \left(1 - \frac{I_{\text{max,Sen}} \cdot N_{\text{sen}}^{\text{HSen}}}{N_{50,\text{Sen}}^{\text{HSen}} + N_{\text{sen}}^{\text{HSen}}} \right) \cdot f_{HFIM}, \tag{8.41}$$

where $IC_{50\text{Sen}0}$ refers to the IC_{50} for a strain with no sensitive alleles, $I_{\text{max,Sen}}$ refers to the maximum fractional decline for IC_{50}, f_{HFIM} refers to the ratio of IC_{50} in the hollow fiber infection model compared with the static time-kill model, and $HSen$ is the hill coefficient.

The MGT is defined as the doubling time required for the bacteria to double in number and is computed from the net growth rate, similar to the computation of half-life (Garrett 1978):

$$MGT = \frac{\ln(2)}{k_{net}}, \tag{8.42}$$

where $k_{net} = k_{growth} - k_{death}$. In the model, the number of resistant alleles (N_{res}) was used as a covariate to compute the MGT (MGT_{12}) wherein k_{12} was computed as $1/MGT_{12}$:

$$MGT_{12} = MGT_0 \cdot \left(1 + \frac{S_{max,Res} \cdot N_{res}^{HRes}}{N_{50,Res}^{HRes} + N_{res}^{HRes}}\right), \tag{8.43}$$

where $N_{50,Res}$ refers to the number of resistant alleles that produce 50% of $S_{max,Res}$, which is the maximum fractional increase in MGT_{12} due to resistant alleles, and *HRes* is the Hill coefficient.

The goal of anti-infective therapy is to administer an effective dose of drug to a patient with a high probability of achieving therapeutic success while minimizing toxicity. Mechanistic models are believed to better describe the processes and subtleties of nature that may not be apparent in an empirical model (Lo et al. 2011). Whether mechanistic models are better predictors of clinical outcome over the empirical and semi-mechanistic models is yet to be proven.

8.3.6 Models of Combination Therapy

We have recently modified the logistic growth model to study the enhanced potency of aztreonam by avibactam using a shift in EC_{50} that approximates the reduction in MIC values at increasing avibactam concentrations against *K. pneumoniae* (Fig. 8.3; Sy et al. 2013). The reduction in aztreonam EC_{50} as a function of avibactam concentration was approximated by an empirical bi-exponential decay equation. Avibactam, being a β-lactamase inhibitor, has no antimicrobial activity against *K. pneumoniae*, but rather restores the potency of aztreonam by inhibiting aztreonam removal and degradation by the β-lactamase enzymes. The advantages of this simple approach are that the model-predicted aztreonam EC_{50} closely mimicked the MIC value and the generated curves described well the observed bacterial dynamics in response to the combination therapy.

The Loewe additivity was utilized to evaluate the effect of combination therapy consisting of a novel aminoglycoside, vertilmicin, and ceftazidime on *P. aeruginosa* (Zhuang et al. 2013). The bacterial population model was based on a two-state logistic growth model. In contrast to the aztreonam–avibactam study, both agents have antimicrobial effects with different mechanisms of action. Greco et al. pro-

posed a generalized sigmoidal E_{max} equation to describe Loewe additivity of the combined effect of two agents (Greco et al. 1995):

$$1 = \frac{C_1}{EC_{50,1}\left(\frac{E_{max}}{E_{max}-k_{max}}\right)^{1/m_1}} \frac{C_2}{EC_{50,2}\left(\frac{E_{max}}{E_{max}-k_{max}}\right)^{1/m_2}} + \frac{\gamma \cdot C_1 \cdot C_2}{EC_{50,1} \cdot EC_{50,2}\left(\frac{E_{max}}{E_{max}-k_{max}}\right)^{(1/2m_1+1/2m_2)}}. \tag{8.44}$$

The additive effect of the two agents is described by the sum of the first two terms and the third term is an interaction term, wherein γ is a parameter that indicates synergism–antagonism interaction. The interaction is additive if the 95% confidence interval of the γ estimate overlaps the zero value. If $\gamma > 0$ or $\gamma < 0$, the interaction is either synergistic or antagonistic, respectively. In the model, m_1 and m_2 were assumed to be equal. An additional interaction term λ was incorporated to the effect of an initial killing rate of both agents (k_{max}) such that:

$$k_{max} = k_{max,1} + k_{max,2} + \lambda \cdot k_{max,1} \cdot k_{max,2}. \tag{8.45}$$

The resulting E_{max} model to evaluate the combination of vertilmicin and ceftazidime was:

$$E_{max} = \frac{k_{max}\left(\frac{C_1}{\alpha_1 EC_{50,1}} + \frac{C_2}{\alpha_2 EC_{50,2}} + \frac{\gamma C_1 C_2}{\alpha_1 \alpha_2 \cdot EC_{50,2} \cdot EC_{50,2}}\right)^k}{1 + \left(\frac{C_1}{\alpha_1 EC_{50,1}} + \frac{C_2}{\alpha_2 EC_{50,2}} + \frac{\gamma C_1 C_2}{\alpha_1 \alpha_2 \cdot EC_{50,2} \cdot EC_{50,2}}\right)^k}, \tag{8.46}$$

where $\propto_i$ refers to the adaptation factor mentioned in Eq. (8.12). This empirical approach described well the combined effects of an aminoglycoside and a β-lactam against *P. aeruginosa*.

8.3.7 Models Estimating Resistant Subpopulation

To quantify the resistant bacterial subpopulation in an *in vitro* time-kill experiment, one can plate the bacteria in agar plates that contained the antimicrobial agent at three times the MIC or greater. This approach ensures that susceptible bacteria are removed by the drug. The choice for at least thrice the MIC is that twice the MIC level is still within the error measurement of susceptibility determination. An alternative method to determine resistance development is to determine the MIC after the 24-h time-kill experiment.

The subpopulation of resistant bacteria is a very small fraction of the total bacterial population that is predominantly drug-susceptible wild-type population. The probability of detecting the resistant subpopulation is dependent on the inoculum size or total bacterial burden and the frequency of mutation to the drug-specific resistance (Jumbe and Drusano 2011). For a resistant subpopulation to amplify effectively, both the fitness of the mutant and the selection pressure presented by the antimicrobial agent are important determining factors. Jumbe and Drusano proposed equations that incorporate probability estimates to a general model that governs the natural replication of bacteria and the death due to antimicrobial effect (Jumbe and Drusano 2011):

$$\frac{dS}{dt} = \zeta_{G,s} \cdot E_{R,s}\left[a(t)\right] \cdot (1-P) S(t) + \zeta_{G,r} \cdot E_{R,r}\left[a(t)\right] \cdot P \cdot \Gamma \cdot R(t) - \Psi_{K,s} \cdot E_{D,s}\left[a(t)\right] \cdot S(t) \tag{8.47}$$

$$\frac{dR}{dt} = \zeta_{G,r} \cdot E_{R,r}\left[a(t)\right] \cdot (1-P) \cdot \Gamma \cdot R(t) + \zeta_{G,s} \cdot E_{R,s}\left[a(t)\right] \cdot P \cdot S(t) - \Psi_{K,r} \cdot E_{D,r}\left[a(t)\right] \cdot R(t), \tag{8.48}$$

where S and R represent susceptible and resistant bacterial population, ζ_G and Ψ_K are rates related to the natural replication and bacterial death, and $E_R a(t)$ and $E_D a(t)$ refer to antimicrobial effects on replication and death. P is the probability related to mutation occurrence and Γ determines the relative fitness of the susceptible to resistant population. This modeling strategy of estimating the proportion of each subpopulation was adopted in the model used to study colistin effect in *P. aeruginosa* that was previously discussed (Bulitta et al. 2010). Tam et al. (2005, 2007b) applied the PKPD model to describe the dynamics of garenoxacin-sensitive and -resistant subpopulations of *P. aeruginosa* and *S. aureus* in response to fluctuating concentrations of quinolone drugs. Their study showed that exposure below a specific breakpoint allowed resistant subpopulation to grow rapidly. Jumbe et al. (2003) showed the predictive value of modeling and simulation in determining the proliferation of resistant population in insufficient antimicrobial therapy.

8.3.8 Models Incorporating Host Defense

Rodent studies provide a good model to evaluate the effect of the host's immune system on the time course of antimicrobial effect by chemotherapeutic agents, as well as the antimicrobial effect imposed by the immune system. The effect of the immune system can be quantified by comparing the immune-competent mice and the neutropenic mice. To evaluate the contribution of granulocytes on bacterial kill, studies performed in the mouse thigh-infection model and the murine model of pneumonia showed that granulocytes alone are potent in eradicating bacteria at a low inoculum size whereas for bacterial burden of $\geq 10^7$ CFU/g of tissue, a net bac-

terial growth was observed after 24 h (Drusano et al. 2010, 2011a, b). The model incorporating host defense has similar mathematical form as that of drug effects and combination study (Jumbe and Drusano 2011):

$$\frac{dN}{dt} = \zeta_G \cdot E_R\left[a(t)\right] \cdot N(t) - C_K \cdot E_D\left[a(t) + E_P + E_P \cdot E_I + E_I\right] \cdot N(t), \quad (8.49)$$

where E_P and E_I refer to the humoral and cellular response of the host and the innate adaptive immunity interaction is characterized by $E_P \cdot E_I$. When the combined effect of the two host's defense processes is greater than the microorganism natural proliferation rate, $C_K >> \zeta_G$, the host immunity can remove the infection without therapeutic intervention (Jumbe and Drusano 2011).

8.3.9 Linking In Vitro Models to PKPD Indices

The concentration–effect relationship of ceftazidime established from *in vitro* time-kill curves was used to explain the PKPD index that $\%fT > \text{MIC}$ of 40 % is required for a static effect *in vivo* (Mouton et al. 2007). The logistic-growth model was used to simulate the bacterial kill over time in dosing regimens of 1 mg every 2 h to 256 mg every 8 h. The pharmacokinetic profiles were simulated using parameters for mice and humans. The dosing regimens that resulted in a predicted static effect (i.e., CFU at 24 h $\leq$ CFU at 0 h) were then evaluated and the corresponding $\%fT > \text{MIC}$ for the dosing regimen was determined. For a 2 $\log_{10}$ decrease after 24 h, the authors estimated that $\%fT > \text{MIC}$ of at least 50 % is required. Neilsen et al. (2011) used a semi-mechanistic PKPD model based on the compartment approach to predict the PKPD indices of several antibiotics. They have shown that simulation studies using the information from *in vitro* studies can be used to predict the PKPD indices of antimicrobial agents but cautioned that the determination of the suitable PKPD index for a particular drug is sensitive to the study conditions including dosing frequency as well as uncertainty in the MIC values.

8.4 Summary

Due to rapid evolution of bacterial resistance to many of the commercially available antimicrobial agents, many investigators have called for drug discovery and development programs that target suppression of resistance selection and eradication of drug-resistant infections (Jumbe and Drusano 2011; Nielsen and Friberg 2013). Pharmacometrics has an important role in developing dosing strategies to effectively achieve these two goals. The search for regimens and drug combinations in anti-infectives has benefitted tremendously from modeling and simulation. Many of the current dosing regimens were based on understanding of the PK–PD relationship between antimicrobial agents and bacterial infection.

In this chapter, we have summarized the pharmacometric models that were used to derive the current state-of-the-art treatment paradigm. More progress can still be made to maximize patients' benefits through implementing treatment programs based on sound analysis of all available information from *in vitro* studies, animal models of infections, and clinical data.

References

Aires JR, Kohler T, Nikaido H, Plesiat P (1999) Involvement of an active efflux system in the natural resistance of *Pseudomonas aeruginosa* to aminoglycosides. Antimicrob Agents Chemother 43:2624–2628

Ambrose PG, Bhavnani SM, Rubino CM, Louie A, Gumbo T, Forrest A, Drusano GL (2007) Pharmacokinetics–pharmacodynamics of antimicrobial therapy: it's not just for mice anymore. Clin Infect Dis 44:79–86

Ambrose PG, Meagher AK, Passarell JA, Van Wart SA, Cirincione BB, Rubino CM, Korth-Bradley JM, Babinchak T, Ellis-Grosse E (2009) Use of a clinically derived exposure–response relationship to evaluate potential tigecycline-Enterobacteriaceae susceptibility breakpoints. Diagn Microbiol Infect Dis 63:38–42

Bakker EP (1992) Aminoglycoside and aminocyclitol antibiotics: hygromycin B is an atypical bactericidal compound that exerts effects on cells of *Escherichia coli* characteristics for bacteriostatic aminocyclitols. J Gen Microbiol 138:563–569

Balaban NQ, Merrin J, Chait R, Kowalik L, Leibler S (2004) Bacterial persistence as a phenotypic switch. Science 305:1622–1625

Bliziotis IA, Samonis G, Vardakas KZ, Chrysanthopoulou S, Falagas ME (2005) Effect of aminoglycoside and beta-lactam combination therapy versus beta-lactam monotherapy on the emergence of antimicrobial resistance: a meta-analysis of randomized, controlled trials. Clin Infect Dis 41:149–158

Breen L, Aswani N (2012) Elective versus symptomatic intravenous antibiotic therapy for cystic fibrosis. Cochrane Database Syst Rev 7:CD002767

Bulitta JB, Ly NS, Yang JC, Forrest A, Jusko WJ, Tsuji BT (2009) Development and qualification of a pharmacodynamic model for the pronounced inoculum effect of ceftazidime against *Pseudomonas aeruginosa*. Antimicrob Agents Chemother 53:46–56

Bulitta JB, Yang JC, Yohonn L, Ly NS, Brown SV, D'hondt RE, Jusko WJ, Forrest A, Tsuji BT (2010) Attenuation of colistin bactericidal activity by high inoculum of *Pseudomonas aeruginosa* characterized by a new mechanism-based population pharmacodynamic model. Antimicrob Agents Chemother 54:2051–2062

Craig WA (1998) Pharmacokinetic/pharmacodynamic parameters: rationale for antibacterial dosing of mice and men. Clin Infect Dis 26:1–10; quiz 11–12

Crandon JL, Schuck VJ, Banevicius MA, Beaudoin ME, Nichols WW, Tanudra MA, Nicolau DP (2012) Comparative in vitro and in vivo efficacies of human simulated doses of ceftazidime and ceftazidime-avibactam against *Pseudomonas aeruginosa*. Antimicrob Agents Chemother 56:6137–6146

Dasgupta A (2007). Usefulness of monitoring free (unbound) concentrations of therapeutic drugs in patient management. Clin Chim Acta 377:1–13

De Kraker ME, Davey PG, Grundmann H (2011) Mortality and hospital stay associated with resistant *Staphylococcus aureus* and *Escherichia coli* bacteremia: estimating the burden of antibiotic resistance in Europe. PLoS Med 8:e1001104

De Kock L, Sy SK, Rosenkranz B, Diacon AH, Prescott K, Hernandez KR, Yu M, Derendorf H, Donald PR (2014) The pharmacokinetics of para-aminosalicylic acid in HIV-uninfected and HIV co-infected tuberculosis patients receiving antiretroviral therapy, managed on multi-

drug-resistant and extensively drug-resistant tuberculosis. Antimicrob Agents Chemother (pii: AAC.03073-14; epub ahead of print)
Drusano GL (2004) Antimicrobial pharmacodynamics: critical interactions of 'bug and drug'. Nat Rev Microbiol 2:289–300
Drusano GL, Preston SL, Hardalo C, Hare R, Banfield C, Andes D, Vesga O, Craig WA (2001) Use of preclinical data for selection of a phase II/III dose for evernimicin and identification of a preclinical MIC breakpoint. Antimicrob Agents Chemother 45:13–22
Drusano GL, Preston SL, Fowler C, Corrado M, Weisinger B, Kahn J (2004) Relationship between fluoroquinolone area under the curve: minimum inhibitory concentration ratio and the probability of eradication of the infecting pathogen, in patients with nosocomial pneumonia. J Infect Dis 189:1590–1597
Drusano GL, Liu W, Fregeau C, Kulawy R, Louie A (2009) Differing effects of combination chemotherapy with meropenem and tobramycin on cell kill and suppression of resistance of wild-type *Pseudomonas aeruginosa* PAO1 and its isogenic MexAB efflux pump-overexpressed mutant. Antimicrob Agents Chemother 53:2266–2273
Drusano GL, Fregeau C, Liu W, Brown DL, Louie A (2010) Impact of burden on granulocyte clearance of bacteria in a mouse thigh infection model. Antimicrob Agents Chemother 54:4368–4372
Drusano GL, Liu W, Kulawy R, Louie A (2011a) Impact of granulocytes on the antimicrobial effect of tedizolid in a mouse thigh infection model. Antimicrob Agents Chemother 55:5300–5305
Drusano GL, Vanscoy B, Liu W, Fikes S, Brown D, Louie A (2011b) Saturability of granulocyte kill of *Pseudomonas aeruginosa* in a murine model of pneumonia. Antimicrob Agents Chemother 55:2693–2695
Dudhani RV, Turnidge JD, Coulthard K, Milne RW, Rayner CR, Li J, Nation RL (2010) Elucidation of the pharmacokinetic/pharmacodynamic determinant of colistin activity against *Pseudomonas aeruginosa* in murine thigh and lung infection models. Antimicrob Agents Chemother 54:1117–1124
Eagle H, Fleischman R, Musselman AD (1950a) Effect of schedule of administration on the therapeutic efficacy of penicillin; importance of the aggregate time penicillin remains at effectively bactericidal levels. Am J Med 9:280–299
Eagle H, Fleischman R, Musselman AD (1950b) The effective concentrations of penicillin in vitro and in vivo for streptococci, pneumococci, and *Treponema pallidum*. J Bacteriol 59:625–643
Eagle H, Fleischman R, Levy M (1953a) "Continuous" vs. "discontinuous" therapy with penicillin; the effect of the interval between injections on therapeutic efficacy. N Engl J Med 248:481–488
Eagle H, Fleischman R, Levy M (1953b) On the duration of penicillin action in relation to its concentration in the serum. J Lab Clin Med 41:122–132
Fisher JF, Meroueh SO, Mobashery S (2005) Bacterial resistance to beta-lactam antibiotics: compelling opportunism, compelling opportunity. Chem Rev 105:395–424
Flume PA, Mogayzel PJ, JR, Robinson KA, Goss CH, Rosenblatt RL, Kuhn RJ, Marshall BC (2009) Cystic fibrosis pulmonary guidelines: treatment of pulmonary exacerbations. Am J Respir Crit Care Med 180:802–808
Garrett ER (1978) Kinetics of antimicrobial action. Scand J Infect Dis 14(Suppl):54–85
Garrett ER, Nolte H (1972) Kinetics and mechanisms of drug action on microorganisms. XIV. The action of fluorouracil, other uracils and derived nucleosides on the microbial kinetics of *Escherichia coli*. Chemotherapy 17:81–108
Garrett ER, Miller GH, Brown MR (1966) Kinetics and mechanisms of action of antibiotics on microorganisms. V. Chloramphenicol and tetracycline affected *Escherichia coli* generation rates. J Pharm Sci 55:593–600
Gershenfeld NA (1999) The nature of mathematical modeling. Cambridge University Press, Cambridge
Grasso S, Meinardi G, De Carneri I, Tamassia V (1978) New in vitro model to study the effect of antibiotic concentration and rate of elimination on antibacterial activity. Antimicrob Agents Chemother 13:570–576

Greco WR, Bravo G, Parsons JC (1995) The search for synergy: a critical review from a response surface perspective. Pharmacol Rev 47:331–385

Hoepelman IM, Rozenberg-Arska M, Verhoef J (1988a) Comparative study of ceftriaxone monotherapy versus a combination regimen of cefuroxime plus gentamicin for treatment of serious bacterial infections: the efficacy, safety and effect on fecal flora. Chemotherapy 34(Suppl 1):21–29

Hoepelman IM, Rozenberg-Arska M, Verhoef J (1988b) Comparison of once daily ceftriaxone with gentamicin plus cefuroxime for treatment of serious bacterial infections. Lancet 1:1305–1309

Hoffman A, Stepensky D (1999) Pharmacodynamic aspects of modes of drug administration for optimization of drug therapy. Crit Rev Ther Drug Carrier Syst 16:571–639

Jorgensen JH, Ferraro MJ (2009) Antimicrobial susceptibility testing: a review of general principles and contemporary practices. Clin Infect Dis 49:1749–1755

Juan C, Moya B, Perez JL, Oliver A (2006) Stepwise upregulation of the *Pseudomonas aeruginosa* chromosomal cephalosporinase conferring high-level beta-lactam resistance involves three AmpD homologues. Antimicrob Agents Chemother 50:1780–1787

Jumbe LNN, Drusano GL (2011) A model-based PK/PD antimicrobial chemotherapy drug development platform to simultaneously combat infectious diseases and drug resistance. In: Kimko HHC, Peck CC (eds) Clinical trial simulations. Springer, New York

Jumbe N, Louie A, Leary R, Liu W, Deziel MR, Tam VH, Bachhawat R, Freeman C, Kahn JB, Bush K, Dudley MN, Miller MH, Drusano GL (2003) Application of a mathematical model to prevent in vivo amplification of antibiotic-resistant bacterial populations during therapy. J Clin Invest 112:275–285

Jumbe NL, Louie A, Miller MH, Liu W, Deziel MR, Tam VH, Bachhawat R, Drusano GL (2006) Quinolone efflux pumps play a central role in emergence of fluoroquinolone resistance in *Streptococcus pneumoniae*. Antimicrob Agents Chemother 50:310–317

Jusko WJ (1971) Pharmacodynamics of chemotherapeutic effects: dose-time-response relationships for phase-nonspecific agents. J Pharm Sci 60:892–895

Kahlmeter G, Brown DF, Goldstein FW, Macgowan AP, Mouton JW, Osterlund A, Rodloff A, Steinbakk M, Urbaskova P, Vatopoulos A (2003) European harmonization of MIC breakpoints for antimicrobial susceptibility testing of bacteria. J Antimicrob Chemother 52:145–148

Kahlmeter G, Brown DF, Goldstein FW, Macgowan AP, Mouton JW, Odenholt I, Rodloff A, Soussy CJ, Steinbakk M, Soriano F, Stetsiouk O (2006) European Committee on Antimicrobial Susceptibility Testing (EUCAST) Technical notes on antimicrobial susceptibility testing. Clin Microbiol Infect 12:501–503

Kullar R, Leonard SN, Davis SL, Delgado G JR, Pogue JM, Wahby KA, Falcione B, Rybak MJ (2011) Validation of the effectiveness of a vancomycin nomogram in achieving target trough concentrations of 15–20 mg/L suggested by the vancomycin consensus guidelines. Pharmacotherapy 31:441–448

Langaee TY, Dargis M, Huletsky A (1998) An ampD gene in *Pseudomonas aeruginosa* encodes a negative regulator of AmpC beta-lactamase expression. Antimicrob Agents Chemother 42:3296–3300

Langaee TY, Gagnon L, Huletsky A (2000) Inactivation of the ampD gene in *Pseudomonas aeruginosa* leads to moderate-basal-level and hyperinducible AmpC beta-lactamase expression. Antimicrob Agents Chemother 44:583–589

Li Y, Peris J, Zhong L, Derendorf H (2006) Microdialysis as a tool in local pharmacodynamics. AAPS J 8:E222–E235

Lo A, Beh J, De Leon H, Hallow MK, Ramakrishna R, Rodrigo M, Sarkar A, Sarangapani R, Georgieva A (2011) Using a systems biology approach to explore hypotheses underlying clinical diversity of the renin angiotensin system and the response to antihypertensive therapies. In: Kimko HHC, Peck CC (eds) Clinical trial simulations. Springer, New York

Louie A, Brown DL, Liu W, Kulawy RW, Deziel MR, Drusano GL (2007) In vitro infection model characterizing the effect of efflux pump inhibition on prevention of resistance to levofloxacin and ciprofloxacin in *Streptococcus pneumoniae*. Antimicrob Agents Chemother 51:3988–4000

Louie A, Liu W, Fikes S, Brown D, Drusano GL (2013) Impact of meropenem in combination with tobramycin in a murine model of *Pseudomonas aeruginosa* pneumonia. Antimicrob Agents Chemother 57:2788–2792

Masuda N, Sakagawa E, Ohya S, Gotoh N, Tsujimoto H, Nishino T (2000a) Contribution of the MexX-MexY-oprM efflux system to intrinsic resistance in *Pseudomonas aeruginosa*. Antimicrob Agents Chemother 44:2242–2246

Masuda N, Sakagawa E, Ohya S, Gotoh N, Tsujimoto H, Nishino T (2000b) Substrate specificities of MexAB-OprM, MexCD-OprJ, and MexXY-oprM efflux pumps in *Pseudomonas aeruginosa*. Antimicrob Agents Chemother 44:3322–3327

Meagher AK, Passarell JA, Cirincione BB, Van Wart SA, Liolios K, Babinchak T, Ellis-Grosse EJ, Ambrose PG (2007) Exposure-response analyses of tigecycline efficacy in patients with complicated skin and skin-structure infections. Antimicrob Agents Chemother 51:1939–1945

Mielck JB, Garrett ER (1969) Kinetics and mechanisms of drug action on microorganisms. IX. Inhibitory action of lincomycin on *Escherichia coli* by microbial kinetics. Chemotherapy 14:337–355

Mine T, Morita Y, Kataoka A, Mizushima T, Tsuchiya T (1999) Expression in *Escherichia coli* of a new multidrug efflux pump, MexXY, from *Pseudomonas aeruginosa*. Antimicrob Agents Chemother 43:415–417

Mohamed AF, Nielsen EI, Cars O, Friberg LE (2012) Pharmacokinetic-pharmacodynamic model for gentamicin and its adaptive resistance with predictions of dosing schedules in newborn infants. Antimicrob Agents Chemother 56:179–188

Moise-Broder PA, Forrest A, Birmingham MC, Schentag JJ (2004a) Pharmacodynamics of vancomycin and other antimicrobials in patients with *Staphylococcus aureus* lower respiratory tract infections. Clin Pharmacokinet 43:925–942

Moise-Broder PA, Sakoulas G, Eliopoulos GM, Schentag JJ, Forrest A, Moellering RC JR (2004b) Accessory gene regulator group II polymorphism in methicillin-resistant *Staphylococcus aureus* is predictive of failure of vancomycin therapy. Clin Infect Dis 38:1700–1705

Mondorf AW, Bonsiepe C, Mondorf W (1989) Randomized multi center study comparing nephrotoxicity of ceftazidime versus the combination of piperacillin and netilmicin with and without furosemide. Adv Exp Med Biol 252:307–312

Mouton JW, Vinks AA (2005) Pharmacokinetic/pharmacodynamic modelling of antibacterials in vitro and in vivo using bacterial growth and kill kinetics: the minimum inhibitory concentration versus stationary concentration. Clin Pharmacokinet 44:201–210

Mouton JW, Vinks AA, Punt NC (1997) Pharmacokinetic-pharmacodynamic modeling of activity of ceftazidime during continuous and intermittent infusion. Antimicrob Agents Chemother 41:733–738

Mouton JW, Punt N, Vinks AA (2005) A retrospective analysis using Monte Carlo simulation to evaluate recommended ceftazidime dosing regimens in healthy volunteers, patients with cystic fibrosis, and patients in the intensive care unit. Clin Ther 27:762–772

Mouton JW, Punt N, Vinks AA (2007) Concentration–effect relationship of ceftazidime explains why the time above the MIC is 40 % for a static effect in vivo. Antimicrob Agents Chemother 51:3449–3451

Mouton JW, Theuretzbacher U, Craig WA, Tulkens PM, Derendorf H, Cars O (2008) Tissue concentrations: do we ever learn? J Antimicrob Chemother 61:235–237

Mouton JW, Ambrose PG, Canton R, Drusano GL, Harbarth S, Macgowan A, Theuretzbacher U, Turnidge J (2011) Conserving antibiotics for the future: new ways to use old and new drugs from a pharmacokinetic and pharmacodynamic perspective. Drug Resist Updates 14:107–117

Mouton JW, Brown DF, Apfalter P, Canton R, Giske CG, Ivanova M, Macgowan AP, Rodloff A, Soussy CJ, Steinbakk M, Kahlmeter G (2012) The role of pharmacokinetics/pharmacodynamics in setting clinical MIC breakpoints: the EUCAST approach. Clin Microbiol Infect 18:E37–E45

Mueller M, De La Pena A, Derendorf H (2004) Issues in pharmacokinetics and pharmacodynamics of anti-infective agents: kill curves versus MIC. Antimicrob Agents Chemother 48:369–377

Nielsen EI, Friberg LE (2013) Pharmacokinetic-pharmacodynamic modeling of antibacterial drugs. Pharmacol Rev 65:1053–1090

Nielsen EI, Viberg A, Lowdin E, Cars O, Karlsson MO, Sandstrom M (2007) Semimechanistic pharmacokinetic/pharmacodynamic model for assessment of activity of antibacterial agents from time-kill curve experiments. Antimicrob Agents Chemother 51:128–136

Nielsen EI, Cars O, Friberg LE (2011) Pharmacokinetic/pharmacodynamic (PK/PD) indices of antibiotics predicted by a semimechanistic PKPD model: a step toward model-based dose optimization. Antimicrob Agents Chemother 55:4619–4630

Nolting A, Dalla Costa T, Rand KH, Derendorf H (1996) Pharmacokinetic-pharmacodynamic modeling of the antibiotic effect of piperacillin in vitro. Pharm Res 13:91–96

Passarell JA, Meagher AK, Liolios K, Cirincione BB, Van Wart SA, Babinchak T, Ellis-Grosse EJ, Ambrose PG (2008) Exposure-response analyses of tigecycline efficacy in patients with complicated intra-abdominal infections. Antimicrob Agents Chemother 52:204–210

Paul M, Benuri-Silbiger I, Soares-Weiser K, Leibovici L (2004) Beta lactam monotherapy versus beta lactam-aminoglycoside combination therapy for sepsis in immunocompetent patients: systematic review and meta-analysis of randomised trials. Br Med J 328:668

Piccart M, Klastersky J, Meunier F, Lagast H, Van Laethem Y, Weerts D (1984) Single-drug versus combination empirical therapy for gram-negative bacillary infections in febrile cancer patients with and without granulocytopenia. Antimicrob Agents Chemother 26:870–875

Poole K, Gotoh N, Tsujimoto H, Zhao Q, Wada A, Yamasaki T, Neshat S, Yamagishi J, Li XZ, Nishino T (1996) Overexpression of the mexC-mexD-oprJ efflux operon in nfxB-type multidrug-resistant strains of *Pseudomonas aeruginosa*. Mol Microbiol 21:713–724

Quale J, Bratu S, Gupta J, Landman D (2006) Interplay of efflux system, ampC, and oprD expression in carbapenem resistance of *Pseudomonas aeruginosa* clinical isolates. Antimicrob Agents Chemother 50:1633–1641

Rybak M, Lomaestro B, Rotschafer JC, Moellering R Jr, Craig W, Billeter M, Dalovisio JR, Levine DP (2009a) Therapeutic monitoring of vancomycin in adult patients: a consensus review of the American Society of Health-System Pharmacists, the Infectious Diseases Society of America, and the Society of Infectious Diseases Pharmacists. Am J Health Syst Pharm 66:82–98

Rybak MJ, Lomaestro BM, Rotschafer JC, Moellering RC, Craig WA, Billeter M, Dalovisio JR, Levine DP (2009b) Vancomycin therapeutic guidelines: a summary of consensus recommendations from the infectious diseases Society of America, the American Society of Health-System Pharmacists, and the Society of Infectious Diseases Pharmacists. Clin Infect Dis 49:325–327

Safdar N, Handelsman J, Maki DG (2004) Does combination antimicrobial therapy reduce mortality in Gram-negative bacteraemia? A meta-analysis. Lancet Infect Dis 4:519–527

Sakoulas G, Moise-Broder PA, Schentag J, Forrest A, Moellering RC Jr, Eliopoulos GM (2004) Relationship of MIC and bactericidal activity to efficacy of vancomycin for treatment of methicillin-resistant Staphylococcus aureus bacteremia. J Clin Microbiol 42:2398–2402

Sanfilippo A, Morvillo E (1968). An experimental model for the study of the antibacterial activity of the sulfonamides. Chemotherapy 13:54–60

Sanfilippo A, Schioppacassi G (1973) New approach to the evaluation of antibacterial activity of aminosidine. Chemotherapy 18:297–303

Schmidt S, Barbour A, Sahre M, Rand KH, Derendorf H (2008) PK/PD: new insights for antibacterial and antiviral applications. Curr Opin Pharmacol 8:549–556

Schmidt S, Sabarinath SN, Barbour A, Abbanat D, Manitpisitkul P, Sha S, Derendorf H (2009) Pharmacokinetic-pharmacodynamic modeling of the in vitro activities of oxazolidinone antimicrobial agents against methicillin-resistant *Staphylococcus aureus*. Antimicrob Agents Chemother 53:5039–5045

Shakil S, Khan R, Zarrilli R, Khan AU (2008) Aminoglycosides versus bacteria—a description of the action, resistance mechanism, and nosocomial battleground. J Biomed Sci 15:5–14

Sideraki V, Huang W, Palzkill T, Gilbert HF (2001) A secondary drug resistance mutation of TEM-1 beta-lactamase that suppresses misfolding and aggregation. Proc Natl Acad Sci U S A 98:283–288

Sobel ML, Mckay GA, Poole K (2003) Contribution of the MexXY multidrug transporter to aminoglycoside resistance in *Pseudomonas aeruginosa* clinical isolates. Antimicrob Agents Chemother 47:3202–3207

Spino M (1991). Pharmacokinetics of drugs in cystic fibrosis. Clin Rev Allergy 9:169–210

Sy SK, Beaudoin ME, Schuck VJ, Derendorf H (2013) Modeling the potentiation of in vitro aztreonam activities by avibactam against four beta-lactam-resistant bacterial strains. Interscience Conference on Antimicrobial Agents and Chemotherapy, Poster A–1014

Tam VH, Louie A, Deziel MR, Liu W, Leary R, Drusano GL (2005) Bacterial-population responses to drug-selective pressure: examination of garenoxacin's effect on *Pseudomonas aeruginosa*. J Infect Dis 192:420–428

Tam VH, Louie A, Deziel MR, Liu W, Drusano GL (2007a) The relationship between quinolone exposures and resistance amplification is characterized by an inverted U: a new paradigm for optimizing pharmacodynamics to counterselect resistance. Antimicrob Agents Chemother 51:744–747

Tam VH, Louie A, Fritsche TR, Deziel M, Liu W, Brown DL, Deshpande L, Leary R, Jones RN, Drusano GL (2007b) Impact of drug-exposure intensity and duration of therapy on the emergence of *Staphylococcus aureus* resistance to a quinolone antimicrobial. J Infect Dis 195:1818–1827

Tam VH, Ledesma KR, Vo G, Kabbara S, Lim TP, Nikolaou M (2008) Pharmacodynamic modeling of aminoglycosides against *Pseudomonas aeruginosa* and *Acinetobacter baumannii*: identifying dosing regimens to suppress resistance development. Antimicrob Agents Chemother 52:3987–3993

Treyaprasert W, Schmidt S, Rand KH, Suvanakoot U, Derendorf H (2007) Pharmacokinetic/pharmacodynamic modeling of in vitro activity of azithromycin against four different bacterial strains. Int J Antimicrob Agents 29:263–270

Tsuji BT, Brown T, Parasrampuria R, Brazeau DA, Forrest A, Kelchlin PA, Holden PN, Peloquin CA, Hanna D, Bulitta JB (2012a) Front-loaded linezolid regimens result in increased killing and suppression of the accessory gene regulator system of *Staphylococcus aureus*. Antimicrob Agents Chemother 56:3712–3719

Tsuji BT, Bulitta JB, Brown T, Forrest A, Kelchlin PA, Holden PN, Peloquin CA, Skerlos L, Hanna D (2012b) Pharmacodynamics of early, high-dose linezolid against vancomycin-resistant enterococci with elevated MICs and pre-existing genetic mutations. J Antimicrob Chemother 67:2182–2190

Vinks AA, Van Rossem RN, Mathot RA, Heijerman HG, Mouton JW (2007). Pharmacokinetics of aztreonam in healthy subjects and patients with cystic fibrosis and evaluation of dose-exposure relationships using monte carlo simulation. Antimicrob Agents Chemother 51:3049–3055

Walkty A, Decorby M, Lagace-Wiens PR, Karlowsky JA, Hoban DJ, Zhanel GG (2011) In vitro activity of ceftazidime combined with NXL104 versus *Pseudomonas aeruginosa* isolates obtained from patients in Canadian hospitals (CANWARD 2009 study). Antimicrob Agents Chemother 55:2992–2994

Wang G, Hindler JF, Ward KW, Bruckner DA (2006) Increased vancomycin MICs for *Staphylococcus aureus* clinical isolates from a university hospital during a 5-year period. J Clin Microbiol 44:3883–3886

Yano Y, Oguma T, Nagata H, Sasaki S (1998) Application of logistic growth model to pharmacodynamic analysis of in vitro bactericidal kinetics. J Pharm Sci 87:1177–1183

Zhuang L, Sy SK, Xia H, Singh RP, Liu C, Derendorf H (2013) Characterization of the in vitro antimicrobial activity of vertilmicin alone and in combination with ceftazidime by using a semi-mechanistic pharmacokinetic/pharmacodynamic model. Interscience Conference on Antimicrobial Agents and Chemotherapy, Poster A-017